

Photomodulation study of partially strained $\text{In}_x\text{Ga}_{1-x}\text{As}$ layers

This article has been downloaded from IOPscience. Please scroll down to see the full text article.

1993 Semicond. Sci. Technol. 8 1420

(<http://iopscience.iop.org/0268-1242/8/7/036>)

View [the table of contents for this issue](#), or go to the [journal homepage](#) for more

Download details:

IP Address: 169.237.79.123

The article was downloaded on 04/02/2013 at 21:35

Please note that [terms and conditions apply](#).

Photomodulation study of partially strained $\text{In}_x\text{Ga}_{1-x}\text{As}$ layers

J H Chen[†], W S Chi[†], Y S Huang[†], Y Yin[‡], F H Pollak[‡], G D Pettit[§]
and J M Woodall[§]

[†] Department of Electronic Engineering, National Taiwan Institute of Technology, Taipei 10772, Taiwan, Republic of China

[‡] Physics Department, Brooklyn College of CUNY, Brooklyn, NY 11210, USA

[§] IBM Thomas J Watson Research Center, Yorktown Heights, NY 10598, USA

Received 19 January 1993, accepted for publication 16 February 1993

Abstract. Photomodulation techniques have been used to study the fundamental transitions of partially strained $\text{In}_x\text{Ga}_{1-x}\text{As}/\text{GaAs}$ ($x = 0.07$ and 0.16) epilayers. The strain-induced splitting of the valence band was observed. The identification of the split valence bands was confirmed using linearly polarized photoreflectance under a total internal reflection mode. The temperature dependence of two bandgap energies E_{01} (heavy-hole band) and E_{02} (light-hole band) was studied over a temperature range from 15 to 300 K. The parameters that describe the temperature dependence of E_{01} and E_{02} as well as the broadening function are evaluated.

1. Introduction

The $\text{In}_x\text{Ga}_{1-x}\text{As}/\text{GaAs}$ system is currently the most promising one for ultrahigh-speed two-dimensional electron gas field-effect transistors because of its small electron effective mass and high electron mobility [1]. It is also used to fabricate quantum confinement heterostructure layers [2], in which the desired optical properties can be achieved by controlling the indium composition and the thickness of layers in the quantum wells. A technological problem results from the fact that $\text{In}_x\text{Ga}_{1-x}\text{As}$ is not lattice-matched to GaAs, leading to compressive strain in the $\text{In}_x\text{Ga}_{1-x}\text{As}$ layers. This strain leads to a tetragonal distortion of the unit cell below a certain critical layer thickness h_c [3]. Above h_c , plastic relaxation occurs increasingly by generation of misfit dislocations. These misfit dislocations greatly affect the physical properties of the material [4, 5]. The lattice parameters of the partly relaxed layer in directions perpendicular and parallel to the surface, a_\perp and a_\parallel , can still differ significantly from the lattice parameters a_0 [3]. The resulting stress affects the energy band structure of the layer, as the bandgap is shifted by an amount δE_H due to the hydrostatic component, and the degeneracy of the $P_{3/2}$ multiplet is split by an amount $2\delta E_S$ due to the shear components [6–8].

This paper presents studies on partially strained $\text{In}_x\text{Ga}_{1-x}\text{As}$ layers grown on (100) GaAs. Using photoreflectance (PR), we observed strain-induced splitting of the valence band energies. The identification of the split valence bands was confirmed using linearly polarized PR

under a total internal reflection mode [9]. The temperature dependence of these two transition energies, E_{01} (heavy hole) and E_{02} (light hole), was carefully studied from 15 to 300 K. We analysed the temperature dependence of E_{01} as well as E_{02} by both Varshni [10] and Bose–Einstein expressions [11–13]. The temperature variation of the broadening parameter Γ has been studied in terms of a Bose–Einstein expression [12, 13]. While both acoustic and optical phonons participate in the energy shift, only the electron–optical phonon interaction is responsible for the changes in linewidth.

2. Theoretical background

When grown on a GaAs buffer the $\text{In}_x\text{Ga}_{1-x}\text{As}$ layers sustain a biaxial in-plane compression and a corresponding extension along the [001] growth direction. The biaxial stress is expected to split the valence band degeneracy [6, 7], by producing anisotropic deformation of the crystal lattice. The asymmetry produced in this manner is similar to that produced by an externally applied uniaxial stress and is expected to have qualitatively the same effect on the energy gap and the valence band splitting [14]. For the E_0 critical points ($\Gamma_6-\Gamma_8$) the hydrostatic component of the strain, δE_H , shifts the valence band of the $\text{In}_x\text{Ga}_{1-x}\text{As}$ relative to the conduction band while the shear component, δE_S , removes the valence band degeneracy, giving a separate E_{01} and E_{02} [6, 7]. If the effect of the strain-induced coupling with the

spin-orbit split band is negligible, the split energy gaps can be expressed in terms of the unstrained value as [8]

$$E_{01} = E_0 + \delta E_H + \delta E_S \quad (1)$$

$$E_{02} = E_0 + \delta E_H - \delta E_S. \quad (2)$$

The values of δE_H and δE_S are given in terms of the strain perpendicular to the (001) surface, ε_z , and the elastic stiffness constants, C_{ij} , by

$$\delta E_H = 2a[(C_{11} - C_{12})/C_{11}]\varepsilon_z \quad (3)$$

$$\delta E_S = -b[(C_{11} + 2C_{12})/C_{11}]\varepsilon_z \quad (4)$$

where a and b are the hydrostatic and tetragonal shear deformation potentials, respectively, and $\varepsilon_z = (a_{\text{GaAs}} - a_{\perp})/a_{\text{GaAs}}$. The value of ε_z can be deduced from the PR data by using the relation

$$\varepsilon_z = \delta E_{\text{split}} / \{-2b[(C_{11} + 2C_{12})/C_{11}]\} \quad (5)$$

where δE_{split} , the split of the heavy-hole and light-hole energy gaps, were determined from the PR measurements. The indium composition was estimated from the growth conditions and the values of the stiffness constants, and the deformation potentials were obtained by interpolating from the values corresponding to the binary compounds listed in table 1.

3. Experimental details

$\text{In}_x\text{Ga}_{1-x}\text{As}$ samples were grown at two nominal compositions, $x = 0.07$ (sample 1), and $x = 0.16$ (sample 2), by molecular beam epitaxy (MBE). The undoped (001) GaAs substrate was degreased, then etched in a solution of H_2SO_4 , H_2O_2 and H_2O , mixed in the ratio of 12:1:1 by volume and quenched in water. When loaded, the substrate was thermally cleaned at 610 °C, and growth of undoped GaAs at $1 \mu\text{m h}^{-1}$ was initiated. The saturated value of the arsenic tetramer beam equivalent pressure was between 15 and 20 times that of the gallium during the growth. Before the 0.4 μm undoped buffer was completed, the substrate temperature was lowered so that the remaining third of the buffer, as well as the 1 μm undoped $\text{In}_x\text{Ga}_{1-x}\text{As}$ and the 100 Å undoped GaAs cap, were grown at 580 °C without interruption or change in source temperature.

The PR apparatus has been described in the literature

[15]. A 1 mW He-Ne laser, chopped at 200 Hz, was used as the modulating source and a 100 W tungsten-halogen lamp filtered by a model 270 McPherson monochromator provided the monochromatic light. The laser intensity was reduced to about 1 to 10% of its initial value by using a neutral-density filter. The reflected light was detected by an EG&G type HUV-2000B silicon photodiode. The normalization of the signal was achieved by an Oriel model 28650 variable neutral-density filter connected to the probe monochromator and the sample. In order to study the polarization dependence of the PR spectra we used an internal reflection mode [9]. The probe beam was introduced through the cleaved (110) side of sample into the GaAs substrate. Thus the K vector of the probe beam was along the [110] direction. Inside the sample the beam propagated almost parallel to the XY plane. It was thus possible to study the spectrum for XY and Z polarizations, where Z is the growth axis. The pumping beam illuminated the sample's surface as in conventional PR experiments. Because of total internal reflection the probe beam was contained inside the sample until reaching the other end. Since the beam traversed the interface region several times before leaving the sample it contained a modulated component carrying information about the properties of the interface region.

4. Results and discussions

Displayed by the dotted curves in figures 1 and 2 are the PR spectra of sample 1 and sample 2 respectively, at 15, 77, 100, 200 and 300 K. The full curves are least-squares fits to the third derivative function (TDF) of a three-dimensional critical point [16]. Here the PR data, $\Delta R/R$ are expressed as a function of the photon energy, E , using the equation

$$\Delta R/R = \sum_{j=1}^2 \text{Re}[A_j \exp(i\theta_j)/(E - E_{0j} + i\Gamma_j)^{2.5}]. \quad (6)$$

The two bandgap energies E_{01} and E_{02} were found along with the amplitude A_j , phase factor θ_j , and broadening parameter Γ_j . The values of E_{0j} obtained from equation (6) are indicated by arrows in figures 1 and 2. The energies E_{01} and E_{02} denote transitions from the conduction band to the valence levels ($J = 3/2, m = \pm 1/2$) and

Table 1. The values of the lattice constants, the stiffness constants, and deformation potentials of GaAs and InAs.

Materials	a_0 (Å)	a (eV)	b (eV)	C_{11} (10^{11} dyn cm $^{-2}$)	C_{12} (10^{11} dyn cm $^{-2}$)
GaAs	5.6533 ^a	- 8.7 ^b	- 2.0 ^b	11.88 ^a	5.32 ^a
InAs	6.0584 ^c	- 5.8 ^d	- 1.8 ^d	8.33 ^c	4.53 ^c

^a From reference [22].

^b From reference [23].

^c From reference [24].

^d From reference [25].

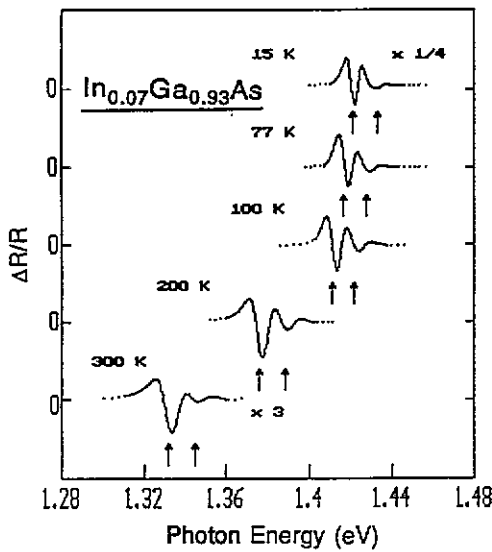


Figure 1. Photoreflectance spectra (dotted curves) of the E_{01} (heavy-hole energy gap) and E_{02} (light-hole energy gap) of the partially strained $\text{In}_{0.07}\text{Ga}_{0.93}\text{As}$ layer at 15, 77, 100, 200 and 300 K. The full curves are least-squares fits to a third-derivative functional form line shape.

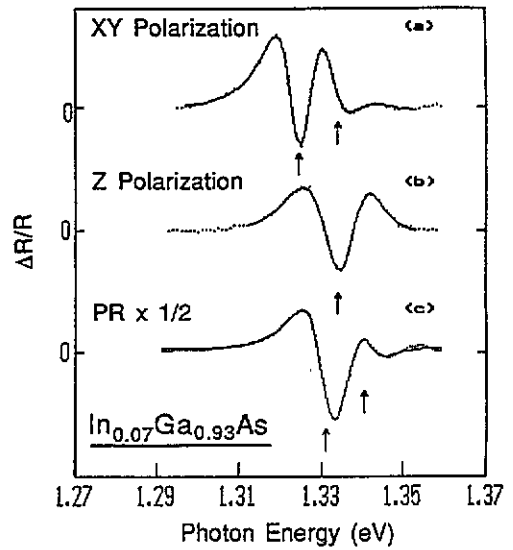


Figure 3. Photoreflectance spectra at 300 K from a partially strained $\text{In}_{0.07}\text{Ga}_{0.93}\text{As}$ layer: (a) photoreflectance in the total internal reflection mode for XY polarization; (b) photoreflectance in the total internal reflection mode for Z polarization; (c) photoreflectance in the conventional mode.

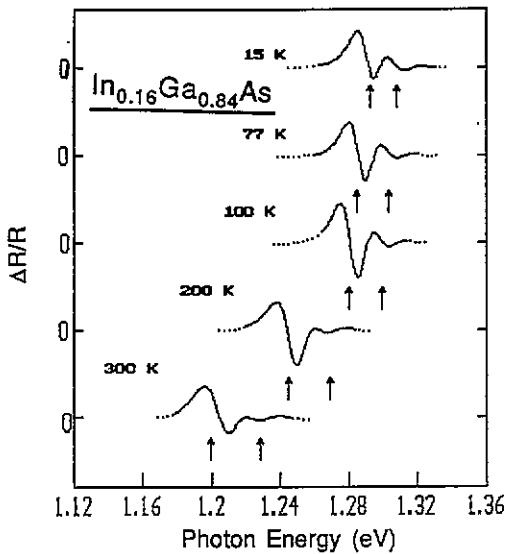


Figure 2. Photoreflectance spectra (dotted curves) of the E_{01} (heavy-hole energy gap) and E_{02} (light-hole energy gap) of the partially strained $\text{In}_{0.16}\text{Ga}_{0.84}\text{As}$ layer at 15, 77, 100, 200 and 300 K. The full curves are least-squares fits to a third-derivative functional form line shape.

($J = 3/2$, $m = \pm 3/2$), respectively. These two features were distinguishable at all temperatures from 15 to 300 K.

The weak features in the higher-energy side of the main structure of PR spectra can also be fitted with Franz-Keldysh oscillations [16, 17]. However, if these features were Franz-Keldysh oscillations, we would expect a smaller number of rapidly damped oscillations at higher temperatures, since the increase in temperature increases the lifetime broadening of the electronic state and decreases the spatial coherence length of the wave-function. In this sense, increasing the temperature has the

effect of localizing the electronic states and thus ultimately destroying the Franz-Keldysh oscillations. But our experimental results indicate that the number of PR features remains the same in the temperature range from 15 to 300 K. It might exclude the possible assignment of Franz-Keldysh oscillations.

From figures 1 and 2, the light-hole band and heavy-hole band are split by $\delta E_{\text{split}} = 13$ meV and 28 meV at room temperature for samples 1 and 2, respectively. The values of strain perpendicular to the (001) surface, ϵ_z , are deduced as -1.76×10^{-3} and -3.80×10^{-3} . These values are less than those of the fully strained layers for the same indium composition obtained by Vegard's law. Table 2 shows the value of δE_{split} and ϵ_z for both samples. For comparison the values of the biaxial strain, ϵ , for the fully strained $\text{In}_x\text{Ga}_{1-x}\text{As}/\text{GaAs}$ (001) layers with same indium composition are included. The results indicate that the strain in the $\text{In}_x\text{Ga}_{1-x}\text{As}$ samples with the thickness of about 1 μm has been partially relieved.

The identification of these features was confirmed using the total internal reflection mode, resulting in the

Table 2. The values of the splitting energy of the light-hole band and the heavy-hole band, δE_{split} , and the deduced strain perpendicular to the (001) surface, ϵ_z , of $\text{In}_x\text{Ga}_{1-x}\text{As}$ ($x = 0.07$ and $x = 0.16$), as well as the biaxial strain, ϵ , for the fully strained layer with the same indium composition.

Materials	δE_{split} (meV)	ϵ_z (10^{-3})	ϵ (10^{-3})
$x = 0.07$	13	-1.757	-5.016
$x = 0.16$	28	-3.801	-11.465

spectra in figures 3 and 4 for polarization of the probe beam in the directions perpendicular and parallel to the (001) surface, respectively. The feature E_{02} is observed for both polarizations. However, the transition corresponding to E_{01} is very weak for Z polarization. Thus, the identifications are unambiguous.

Figures 3 and 4 show that the transition energies determined from total internal reflection mode are lower than those from PR measurement, and that the broadening parameters are much larger for the total internal reflection measurements. This difference might indicate the non-uniform relaxation of the thick $\text{In}_x\text{Ga}_{1-x}\text{As}$ epilayers. For the total internal reflection mode, the beam traversed the interface region several times before leaving the sample; it contained information mostly about the properties of the interface region, while the information obtained from PR is from the region that the probe beam can penetrate. The larger value of the broadening parameter determined from the total internal reflection mode is probably related to the relatively high concentration of misfit dislocations associated with the partial strain relief in the interface region.

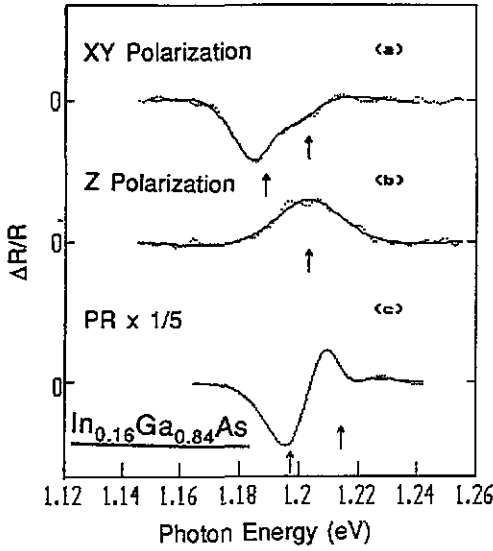


Figure 4. Photoreflectance spectra at 300 K from a partially strained $\text{In}_{0.16}\text{Ga}_{0.84}\text{As}$ layer: (a) photoreflectance in the total internal reflection mode for XY polarization; (b) photoreflectance in the total internal reflection mode for Z polarization; (c) photoreflectance in the conventional mode.

Plotted in figure 5 are the temperature variations of E_{01} and E_{02} for the sample 1 and sample 2, respectively. Representative error bars are shown. The full curves are least-squares fits to the Varshni semiempirical relationship [10]

$$E_{0i}(T) = E_{0i}(0) - \alpha T^2/(\beta + T). \quad (7)$$

The obtained values of $E_{0i}(0)$, α and β for both samples are listed in table 3. For comparison, we have also listed in table 3 the values of $E_0(0)$, α and β of the direct gap (E_0) for GaAs obtained by previous investigators [18]. There are slight differences in estimates of α and β for the light- and heavy-hole gaps. Since the differences are within the probable errors of measurement, a detailed comparison of these parameters is difficult to make. The values α and β are found to be similar to those of GaAs because of the low indium concentration of the layers. The data have also been fitted to the Bose-Einstein expression given by Lautenschlager *et al* [11, 12]:

$$E_{0i}(T) = E_B - a_B \{1 + 2/[\exp(\Theta_B/T) - 1]\} \quad (8)$$

where a_B represents the strength of the electron-phonon interaction and Θ_B corresponds to the average phonon temperature. Both electron-optical phonon and electron-acoustic phonon interactions contribute to the shift

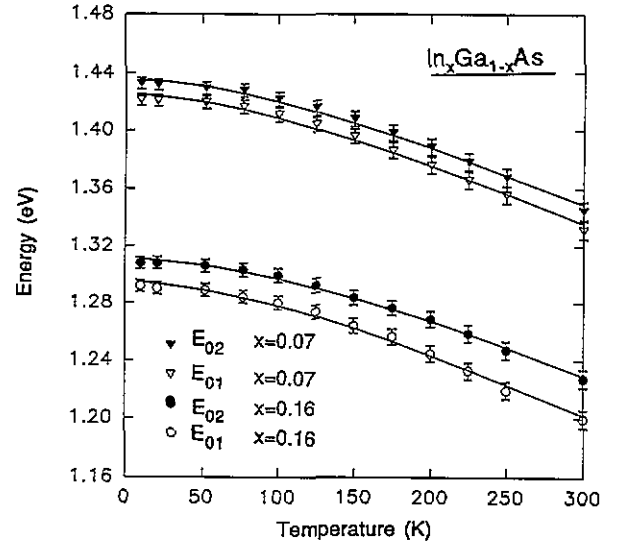


Figure 5. The temperature dependence of E_{01} and E_{02} of $\text{In}_x\text{Ga}_{1-x}\text{As}$ for $x = 0.07$ and $x = 0.16$. The full curves are least-squares fits to $E_{0i}(T) = E_{0i}(0) - \alpha T^2/(\beta + T)$.

Table 3. Values of the parameters which describe the temperature dependence of E_{01} and E_{02} of $\text{In}_x\text{Ga}_{1-x}\text{As}$ ($x = 0.07$ and $x = 0.16$) and GaAs.

Materials	$E_{0i}(0)$ (eV)	α (10^{-4} eV K $^{-1}$)	β (K)	E_B (eV)	a_B (meV)	Θ_B (K)
$x = 0.07$	E_{01}	1.425 ± 0.005	4.8 ± 0.4	196 ± 40	1.468 ± 0.014	45 ± 9
	E_{02}	1.436 ± 0.005	5.0 ± 0.4	210 ± 40	1.479 ± 0.014	47 ± 9
$x = 0.16$	E_{01}	1.295 ± 0.005	5.1 ± 0.4	200 ± 50	1.347 ± 0.015	53 ± 10
	E_{02}	1.311 ± 0.005	5.3 ± 0.4	271 ± 50	1.363 ± 0.015	55 ± 10
GaAs	1.517 ± 0.008^a	5.5 ± 1.3^a	225 ± 174^a	1.571 ± 0.023^a	57 ± 29^a	240 ± 102^a

^aFrom reference [19].

Table 4. Parameters involved in the temperature dependence of the broadening parameter of E_{01} and E_{02} of $\text{In}_x\text{Ga}_{1-x}\text{As}$ ($x = 0.07$ and $x = 0.16$) using the fit $\Gamma_i(T) = \Gamma_{0i} + \Gamma_{1i}/[\exp(\Theta_i/T) - 1]$.

Materials	$\Theta_{\text{LO}1}$ (K)	$\Theta_{\text{LO}2}$ (K)	Γ_{0i} (meV)	Γ_{1i} (meV)	Θ_i (K)
$x = 0.07$	410 ^a	376 ^a	$\Gamma_{01} = 4.8 \pm 0.2$ $\Gamma_{02} = 4.1 \pm 0.2$	$\Gamma_{11} = 17 \pm 5$ $\Gamma_{12} = 17 \pm 5$	$\Theta_1 = 495 \pm 120$ $\Theta_2 = 515 \pm 120$
$x = 0.16$	406 ^a	375 ^a	$\Gamma_{01} = 8.6 \pm 0.3$ $\Gamma_{02} = 7.4 \pm 0.3$	$\Gamma_{11} = 22 \pm 6$ $\Gamma_{12} = 22 \pm 6$	$\Theta_1 = 366 \pm 120$ $\Theta_2 = 468 \pm 120$

^a Longitudinal optical phonon temperatures for the ‘GaAs-like’ ($\Theta_{\text{LO}1}$) and ‘InAs-like’ ($\Theta_{\text{LO}2}$) modes of $\text{In}_x\text{Ga}_{1-x}\text{As}$ obtained from Raman measurements.

of E_{01} and E_{02} [11, 19]. Our values for E_B , a_B and Θ_B are given in table 3; also listed are the corresponding values for the direct gap of GaAs [19]. The values of a_B and Θ_B for E_{01} and E_{02} are slightly different for both samples. In order to have a better understanding of this difference, detailed studies on the fully strained samples over a much wider temperature range is desirable. In addition, the effects due to the difference in temperature dependences of the expansion coefficients of substrate and epilayer materials also need to be considered.

The temperature dependence of broadening parameter of E_{01} and E_{02} for sample 1 and sample 2 are displayed in figure 6 (error bars are shown). The full curves are least-squares fits to the equation [12, 19]

$$\Gamma_i(T) = \Gamma_{0i} + \Gamma_{1i}/[\exp(\Theta_i/T) - 1]. \quad (9)$$

The values of Γ_{0i} , Γ_{1i} and Θ_i corresponding to the broadening parameter of E_{01} and E_{02} are listed in table 4. The first term of equation (9) contains inhomogeneous contributions due to interface roughness, dislocations, alloy scattering or strain distributions. The obtained value of Γ_{0i} for the $x = 0.16$ sample is larger than that for the $x = 0.07$ sample and both are significantly greater

than that expected from alloy scattering of about 2 meV [20]. These results are probably related to the relatively high concentration of misfit dislocations associated with the partial strain relief. The second term of equation (9) corresponds to the lifetime broadening due to the electron-optical phonon interaction. The quantity Γ_{1i} represents the strength of the electron-optical phonon coupling while Θ_i is the optical phonon temperature. For comparison the longitudinal optical (LO) phonon temperatures for the ‘GaAs-like’ ($\Theta_{\text{LO}1}$) and ‘InAs-like’ ($\Theta_{\text{LO}2}$) modes of these two samples, obtained from Raman measurements, are presented in table 4. The Θ_i values are quite close to $\Theta_{\text{LO}1}$ and $\Theta_{\text{LO}2}$ for both samples. Since Θ_i for both samples is quite similar to the LO phonon temperature ($\Theta_{\text{LO}1}$ and $\Theta_{\text{LO}2}$). The temperature variation of Γ_i is due mainly to the interaction of the electron with optical phonons. These observations are in agreement with existing theory [13, 21].

5. Conclusion

In conclusion, we have studied the fundamental transitions of partially strained $\text{In}_x\text{Ga}_{1-x}\text{As}/\text{GaAs}$ epilayers by photomodulation techniques. The strain-induced splitting of the valence band is observed. The identification of the split valence bands was confirmed using linearly polarized PR under a total internal reflection mode. The temperature dependence of these two transition energies E_{01} and E_{02} is carefully studied from 15 to 300 K. We have analysed $E_{01}(T)$ and $E_{02}(T)$ in terms of both Varshni and Bose-Einstein expressions, while the temperature variation of $\Gamma(T)$ has been fitted with a Bose-Einstein equation. Both optical and acoustic phonons contribute to the shift of E_{01} and E_{02} ; only optical phonons participate in the temperature variation of the broadening function.

Acknowledgments

J H Chen, W S Chi and Y S Huang acknowledge the support of the National Science Council of the Republic of China. Y Yin and F H Pollak acknowledge the partial support of US Army Research Office contract #DAAL03-92-G-0189.

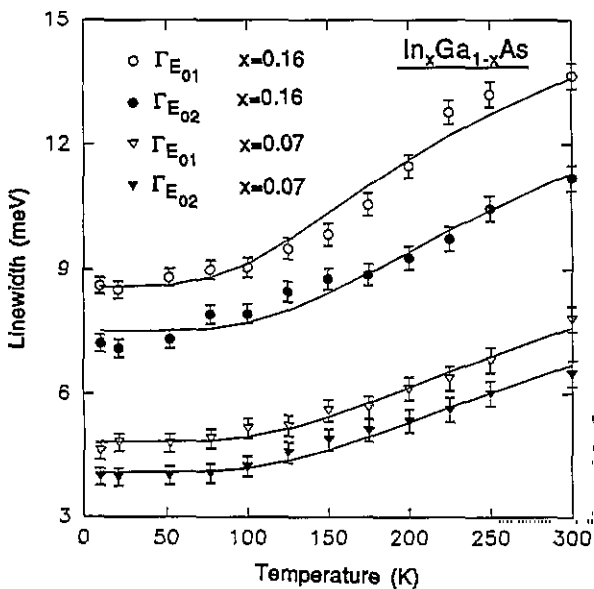


Figure 6. The temperature variation of the broadening parameters of E_{01} and E_{02} of $\text{In}_x\text{Ga}_{1-x}\text{As}$ for $x = 0.07$ and $x = 0.16$. The full curves are least-squares fits to $\Gamma_i(T) = \Gamma_{0i} + \Gamma_{1i}/[\exp(\Theta_i/T) - 1]$.

References

- [1] Nguyen L D, Radulescu D C, Foisy M C, Tasker J and Eastman L F 1989 *IEEE Trans. Electron Devices* **36** 833
- [2] Tsang W T 1987 *Semiconductor and Semimetals* vol 24 ed R Dingle (New York: Academic) p 397
- [3] Matthews J W and Blakeslee A E 1974 *J. Crystal Growth* **27** 118
- [4] Grundmann M, Christen J, Bimberg D, Fischer-Colbrie A and Hull R 1989 *J. Appl. Phys.* **66** 2214
- [5] Grundmann M, Lienert U, Bimberg D, Fischer-Colbrie A and Miller J N 1989 *Appl. Phys. Lett.* **55** 1765
- [6] Pollak F H and Cardona M 1968 *Phys. Rev.* **172** 816
- [7] Pollak F H 1973 *Surf. Sci.* **37** 863
- [8] Flemish J R, Shen H, Jones K A, Dutta M and Ban V S 1991 *J. Appl. Phys.* **70** 2152
- [9] Ksendzov A, Shen H, Pollak F H and Bour D P 1990 *Solid State Commun.* **73** 11
- [10] Varshni Y P 1967 *Physica* **34** 149
- [11] Lautenschlager P, Garriga M and Cardona M 1987 *Phys. Rev. B* **36** 4813
- [12] Lautenschlager P, Garriga M, Vina L and Cardona M 1987 *Phys. Rev. B* **36** 4821
- [13] Gopalan S, Lautenschlager P and Cardona M 1987 *Phys. Rev. B* **35** 5577
- [14] Kuo C P, Vong S K, Cohen R M and Stringfellow G B 1985 *J. Appl. Phys.* **57** 5428
- [15] Shen H, Parayanthal P, Lin Y F and Pollak F H 1987 *Rev. Sci. Instrum.* **58** 1429
- [16] Aspnes D E 1980 *Handbook on Semiconductors* vol 2 ed T S Moss (New York: North-Holland) p 109
- [17] Shen H and Pollak F H 1990 *Phys. Rev. B* **42** 7097
- [18] Shen H, Pan S H, Hang Z, Leng J, Pollak F H, Woodall J M and Sacks R N 1988 *Appl. Phys. Lett.* **53** 1080
- [19] Lautenschlager P, Garriga M, Logothetidis S and Cardona M 1987 *Phys. Rev. B* **35** 9174
- [20] Singh J and Bajaj K K 1986 *Appl. Phys. Lett.* **48** 1077
- [21] Allen P B and Cardona M 1981 *Phys. Rev. B* **23** 1495
- [22] Adachi S 1985 *J. Appl. Phys.* **58** R1
- [23] Qiang H, Pollak F H and Hickman G 1990 *Solid State Commun.* **76** 1087
- [24] Adachi S 1982 *J. Appl. Phys.* **53** 8775
- [25] Hellwege K H (ed) 1982 *Landolt-Börnstein New Series Group III* vol 179 (Berlin: Springer)